ISSN 1949-8470 (online)

World Journal of *Radiology*

*World J Radiol*2023 February 28; 15(2): 32-55

Published byBaishideng Publishing Group Inc

WJR World Journal of Radiology

Contents

Monthly Volume 15 Number 2 February 28, 2023

World Journal of Radiology

Monthly Volume 15 Number 2 February 28, 2023

Contents

ABOUT COVER

Editorial Board Member of *World Journal of Radiology*, Mustafa Z Mahmoud, PhD, Adjunct Professor, Full Professor, Radiology and Medical Imaging Department, Prince Sattam bin Abdulaziz University, Al-Kharj 11942, Saudi Arabia. zuhairmustafa4@hotmail.com

AIMS AND SCOPE

The primary aim of *World Journal of Radiology* (*WJR*, *World J Radiol*) is to provide scholars and readers from various fields of radiology with a platform to publish high-quality basic and clinical research articles and communicate their research findings online.

WJR mainly publishes articles reporting research results and findings obtained in the field of radiology and covering a wide range of topics including state of the art information on cardiopulmonary imaging, gastrointestinal imaging, genitourinary imaging, musculoskeletal imaging, neuroradiology/head and neck imaging, nuclear medicine and molecular imaging, pediatric imaging, vascular and interventional radiology, and women's imaging.

INDEXING/ABSTRACTING

The *WJR* is now abstracted and indexed in PubMed, PubMed Central, Emerging Sources Citation Index (Web of Science), Reference Citation Analysis, China National Knowledge Infrastructure, China Science and Technology Journal Database, and Superstar Journals Database. The 2022 edition of Journal Citation Reports ® cites the 2021 Journal Citation Indicator (JCI) for *WJR* as 0.48.

RESPONSIBLE EDITORS FOR THIS ISSUE

Production Editor:*Si Zhao*; **Production Department Director:***Xu Guo*; **Editorial Office Director:***Jia-Ru Fan*.

NAME OF JOURNAL
World Journal of Radiology

ISSN
ISSN 1949-8470 (online)

LAUNCH DATE
January 31, 2009

FREQUENCY
Monthly

EDITORS-IN-CHIEF
Thomas J Vogl

EDITORIAL BOARD MEMBERS
https://www.wjgnet.com/1949-8470/editorialboard.htm

PUBLICATION DATE
February 28, 2023

INSTRUCTIONS TO AUTHORS
https://www.wjgnet.com/bpg/gerinfo/204

GUIDELINES FOR ETHICS DOCUMENTS
https://www.wjgnet.com/bpg/GerInfo/287

GUIDELINES FOR NON-NATIVE SPEAKERS OF ENGLISH
https://www.wjgnet.com/bpg/gerinfo/240

PUBLICATION ETHICS
https://www.wjgnet.com/bpg/GerInfo/288

PUBLICATION MISCONDUCT
https://www.wjgnet.com/bpg/gerinfo/208

ARTICLE PROCESSING CHARGE
https://www.wjgnet.com/bpg/gerinfo/242

STEPS FOR SUBMITTING MANUSCRIPTS
https://www.wjgnet.com/bpg/GerInfo/239

ONLINE SUBMISSION
https://www.f6publishing.com

World Journal of Radiology

Submit a Manuscript: https://www.f6publishing.com

World J Radiol 2023 February 28; 15(2): 32-41

DOI: 10.4329/wjr.v15.i2.32

ISSN 1949-8470 (online)

ORIGINAL ARTICLE

Prospective Study

Effects of combining multiple dose reduction techniques on coronary computed tomography angiography

Xiao-Lu Hu, Pei-Kai Huang, Meng Zhang, Jun Chen, Meng-Qiang Xiao

Specialty type: Radiology, nuclear medicine and medical imaging

Provenance and peer review: Unsolicited article; Externally peer reviewed.

Peer-review model: Single blind

Peer-review report's scientific quality classification

Grade A (Excellent): 0
Grade B (Very good): B
Grade C (Good): C
Grade D (Fair): D
Grade E (Poor): 0

P-Reviewer: Crocé LS, Italy; El-Serafy AS, Egypt; Shariati MBH, Iran

Received: May 29, 2022
Peer-review started: May 29, 2022
First decision: August 22, 2022
Revised: September 23, 2022
Accepted: February 13, 2023
Article in press: February 13, 2023
Published online: February 28, 2023

Xiao-Lu Hu, Pei-Kai Huang, Meng Zhang, Jun Chen, Meng-Qiang Xiao, Department of Imaging, Zhuhai Hospital, Guangdong Provincial Hospital of Traditional Chinese Medicine, Zhuhai 650031, Guangdong Province, China

Corresponding author: Meng-Qiang Xiao, Doctor, Deputy Doctor, Department of Imaging, Zhuhai Hospital, Guangdong Provincial Hospital of Traditional Chinese Medicine, No. 53 Jingle Road, Zhuhai 650031, Guangdong Province, China. xmqzhuhai@163.com

Abstract

BACKGROUND

Coronary computed tomography angiography (CCTA) is the preferred non-invasive examination method for coronary heart disease. However, the radiation from computed tomography has become a concern since public awareness of radiation hazards continue to increase.

AIM

To explore the value of multiple dose reduction techniques for CCTA.

METHODS

Consecutive normal and overweight patients were prospectively divided into two groups: Group A_1, patients who received multiple dose reduction scans (n = 82); and group A_2, patients who received conventional scans (n = 39). The scan parameters for group A_1 were as follows: Isocentric scan, tube voltage = 80 kV, and tube current control using 80% smart milliampere. The scan parameters for group A_2 were as follows: Normal position, tube voltage = 100 kV, and smart milliampere.

RESULTS

The average effective doses (EDs) for groups A_1 and A_2 were 1.13 ± 0.35 and 3.36 ± 1.30 mSv, respectively. There was a statistically significant difference in ED between the two groups (P < 0.01). Furthermore, noise was significantly lower, and both signal-to-noise ratio and contrast signal-to-noise ratio were higher in group A_2 when compared to group A_1 (P < 0.01). Moreover, the subjective image quality (IQ) scores were excellent in both groups, in which there was no significant difference in subjective IQ score between the two groups (P = 0.12).

CONCLUSION

Multiple dose reduction scan techniques can significantly decrease the ED of

patients receiving CCTA examinations for clinical diagnosis.

Key Words: Isocentric scanning; Coronary heart disease; Dose reduction techniques; Coronary computed tomography angiography; Radiation

Core Tip: Coronary computed tomography angiography (CCTA) is the preferred non-invasive examination method for coronary heart disease (CHD). The present study was the first to combine multiple dose reduction techniques, including narrow acquisition window, low tube voltage, lower tube current, and isocentric scanning, to decrease CCTA radiation exposure of patients with suspected CHD. The radiation dose for the group with multiple dose reduction was approximately 33.63% (1.13 ± 0.35/3.36 ± 1.30) of the dose associated with the conventional method.

Citation: Hu XL, Huang PK, Zhang M, Chen J, Xiao MQ. Effects of combining multiple dose reduction techniques on coronary computed tomography angiography. *World J Radiol* 2023; 15(2): 32-41
URL: https://www.wjgnet.com/1949-8470/full/v15/i2/32.htm
DOI: https://dx.doi.org/10.4329/wjr.v15.i2.32

INTRODUCTION

Coronary computed tomography angiography (CCTA) is the preferable non-invasive method to check for coronary heart disease (CHD)[1,2]. In terms of technology, CCTA has advanced significantly during the last 20 years. For those who suspect they may have CHD, CCTA has largely taken the role of conventional invasive coronary angiography since it is so effective at detecting moderate to severe coronary artery stenosis[2]. But as individuals become increasingly conscious of the risks associated with radiation, computed tomography (CT) radiation has risen to the forefront of discussion[3].

Numerous dose-reduction techniques have been developed as a result of the advancement of computer technology, including prospective electrocardiography gating, iterative reconstruction, personalized scanning, as well as "smart milliampere" (the CT can automatically calculate the tube current based on the position scan) have been developed[3,4]. Furthermore, with the emergence of high-end CT machines, adjusting the tube voltage and tube current has become a useful approach for dose reduction in CCTA scanning[1,5,6]. Some organizations have reported the application of dual-source CT (Siemens Healthcare, Malvern, PA, United States) and GE gem energy spectrum CT (Medical Systems, Milwaukee, WI, United States) to reduce the tube voltage to 80 kV and manage the tube current with smart milliamperes, thereby decreasing the effective dose (ED) to a significant degree[7,8]. Furthermore, previous researchers have employed single dose reduction techniques to minimize the CCTA radiation dose. However, there are limitations in reducing the overall ED. Therefore, more advanced methods are warranted to further decrease the radiation exposure during CCTA.

Isocentric scanning has been proven as an effective approach to reduce radiation exposure in patients receiving CCTA examinations[9,10]. The direction of the beam in the CT is fixed in the middle of the CT frame. The beam in multislice spiral CT has a cone-like form. More light would reach the system through a spherical tube and frame-hole-center-scanning detector, which would enhance the quality of the objective picture [image quality (IQ)]. When an object is being scanned isocentrically, it aligns with the gantry's empty center. This technology has been heavily utilized by all varieties of CT. Additionally, it has been shown that using this technique in CT may lower the ED of scans for organs that are not in the middle[11,12].

To our knowledge, the present study was the first to combine multiple dose reduction techniques, including narrow acquisition window, low tube voltage, lower tube current, and isocentric scanning, in order to decrease the CCTA radiation exposure of patients with suspected CHD. The present study aimed to determine whether multiple dose reduction approaches can efficiently reduce the radiation exposure while maintaining the IQ in CCTA examinations.

MATERIALS AND METHODS

Study population

The present prospective research was approved by the institutional review board of Guangdong Provincial Hospital of Traditional Chinese Medicine Medical Ethics Committee (BF2020-229-01), and all

patients provided written informed consent. Between November 2020 and August 2021, consecutive patients with clinically suspected CHD were screened for inclusion in the present study. The inclusion criteria were as follows: Age ≥ 18-years-old; heart rate < 70 bpm; and body mass index (BMI): 18.0-29.9 kg/m^2. Patients with pacemakers, severe respiratory artifacts, metal implants within the scan range, allergies to contrast media or Betaloc, or a history of cardiac tumors or cardiac surgery were excluded.

The study population comprised 118 patients with CHD. These patients were classified according to their BMI, as described above, and divided into two groups [the groups were classified as normal or overweight (BMI: 18.0-29.9 kg/m^2)[13], BMI = weight (kg)/height (m)^2]: Multi-modality normal group (group A_1, n = 82) and conventional normal group (group A_2, n = 39). Coronary artery segmentation was performed according to the 15-segment coronary artery segmentation method developed by the American Heart Association[1].

CCTA examination

The CCTA examination was performed using the Canon 320-row dynamic CT system (Aquilion ONE Genesis, Canon Medical Systems). Prospective electrocardiography gating was used to reduce the radiation dose[6]. The scanning range was extended 140 mm upwards, starting from the lower edge of the heart. For group A_1, the isocentric scan was performed with the patient supine and their body shifted to the right (Figure 1). Before the CCTA scan, an ultrasound examination was performed to mark the leftmost and rightmost edges of the heart on the body surface, and perpendicular lines were placed along the leftmost and rightmost edges of the heart. The centerline of the two vertical lines was used as the vertical positioning line, and the horizontal axillary centerline was used as the horizontal positioning line.

Patients in group A_2 were scanned using the conventional method, with the patient placed in the natural supine position. Similarly, the horizontal axillary centerline was used for the horizontal positioning, and the median line was used as the vertical positioning line. The scan parameters were as follows: Group A_1, tube voltage = 80 kV, 80% tube current, smart milliampere setting; group A_2, tube voltage = 100 kV, tube current control using milliampere (Table 1).

Preparations before scanning

All patients provided a written informed consent before participating in the study. Heart rate and blood pressure were measured at rest before the examination. Patients with a heart rate of > 70 bpm were given metoprolol (Betaloc, 25-100 mg). These patients were randomly assigned into two groups (groups A_1 and A_2) at a ratio of 2:1. Before the examination, these patients were administered with 0.5 mg nitroglycerine tablets.

Radiation dose

The CT dose index volume (mGy) and dose length product (mGy × cm) were automatically calculated by the scanner software for all CT protocols. Then, the dose length product was multiplied by a conversion coefficient (k) to determine the ED (ED = dose length product × k, k = 0.014)[13] for each patient (Table 2).

Image processing

All images were reconstructed using Adaptive Iterative Dose Reduction Using Three Dimensional Processing. The scanning parameters were as follows: Scan length, 140 mm; slice thickness, 0.5 mm; reconstruction field of view, 220 mm; kernel, EU10 (Table 2).

Subjective and objective evaluation of IQ

The objective IQ was evaluated by two experienced cardiovascular radiologists (MQ Xiao, 17 years of experience; PK Huang, 13 years of experience), who were blinded to the scan and reconstruction parameters. A circular region of interest (ROI), with a diameter of 1 cm, was placed within the cortical part of the main bronchus. The coronary artery attenuation values for the proximal ROIs of the left main coronary artery and right coronary artery were measured. The ROI was selected as large as possible, and the vascular wall, vascular calcifications, and non-calcified plaques and artifacts were excluded. The average coronary artery attenuation was equal to the average value of the left main coronary artery and proximal right coronary artery. The ROI measurement was performed on the adjacent myocardial fat. This was repeated three times at each location, and averaged to ensure data consistency. The CT value standard deviation for the main bronchus, and average attenuation values for the coronary artery and pericardial fat were calculated by averaging the values obtained by the two observers. Noise was calculated as the standard deviation of the CT value of the main bronchus[14]. The signal-to-noise ratio and contrast signal-to-noise ratio (CNR) were calculated as follows: Signal-to-noise ratio = average main bronchus CT value/image noise; CNR = (average attenuation of coronary artery - perivascular fat attenuation)/image noise[15].

Coronary artery segmentation was performed according to the 15-segment coronary artery segmentation method developed by the American Heart Association[1]. Two radiologists with 18 years (MQ Xiao) and 13 years (PK Huang) of experience in cardiovascular medicine conducted independent

Table 1 Computed tomography parameters for the conventional and multi-modality treatment groups

Dose group	Conventional group	Multi-modality group
Tube voltage, kV	100	80
Tube current, mA	Smart milliampere	80% smart milliampere
D-FOV, mm	220	220
Rotation time, s	0.275	0.275
Thickness, mm	0.5	0.5
Interval, mm	0.5	0.5
AIDR3D	Standard EU10	Standard EU10
Scanning method	ECG gating	ECG gating
Cardiac cycle	30%-80%	60%-80%
Scan position	Conventional	Isocentric
Scan length	140 mm	140 mm

AIDR3D: Adaptive Iterative Dose Reduction Using Three Dimensional Processing; ECG: Electrocardiography.

Table 2 Characteristics of the two groups

Group, *n*	Sex, F/M	Age, yr	BMI, kg/m^2	CTD_{vol}, mGy	DLP, mGy × cm	ED, mSv
A_1, *n* = 82	31/51	59.59 ± 9.66	23.06 ± 1.95	5.89 ± 1.85	80.58 ± 24.80	1.13 ± 0.36
A_2, *n* = 36	19/20	64.15 ± 13.28	22.58 ± 1.96	17.92 ± 8.02	250.90 ± 112.25	3.36 ± 1.30
P value	0.43	0.17	0.89	0.00	0.00	0.00

BMI: Body mass index; CTD_{vol}: Computed tomography dose index volume; DLP: Dose length product; ED: Effective dose; F: Female; M: Male.

evaluations for coronary arteries with a diameter of ≥ 1.5 mm. For inter-rater disagreements, a consensus was reached through consultation. Furthermore, a 5-point Likert scale was used[13] as follows: 5 = excellent (sharp, smooth contours of the vascular wall and no streaking or radiating artifacts); 4 = good (slight irregularities on the contours and few streaks or radiating artifacts); 3 = fair (blurred and irregular contour of the vascular wall and numerous streaks or radiating artifacts); 2 = poor (deformation of the vascular wall and various artifacts); 1 = very poor (obvious deformation of the vascular wall and extensive artifacts). Images with IQ scores of 3-5 satisfied the requirements for the diagnostic assessment (Figure 2).

RESULTS

The study population comprised 118 patients (71 male and 47 female patients), who were within 37-87-years-old (mean ± SD: 61.06 ± 9.10 years).

These normal and overweight patients were divided into two groups: Group A_1, patients who underwent multiple dose reduction scan techniques (*n* = 82); and group A_2, patients who underwent the conventional scan technique (*n* = 39). Sex, age, and BMI did not significantly vary across the groups (*P* is between 0.06 and 0.43; Table 2).

The average ED of group A_1 was 1.13 ± 0.35 mSv, whereas the average ED of group A_2 was 3.36 ± 1.30 mSv. The difference between the ED of these two groups was statistically significant (all *P* less than 0.01). Additionally, the average noise in group A_2 was much lower than group A_1 (all *P* more than 0.05; Table 3), and the signal-to-noise ratio and CNR in group A_2 were significantly higher than group A_1. Additionally, group A_1 had considerably higher CT values than group A_2 for the right coronary artery root, left main coronary artery, and ascending aortic root (*P* less than 0.05).

There was a total of 1603 potentially evaluable segments. Among these, in the 100 kV group, 40 segments were deemed unevaluable, and in the 80 kV group, 49 segments were deemed unevaluable due to having a diameter of < 1.5 mm or occlusion. The statistics for the coronary artery segments in groups A_1 and A_2 were presented in Table 2. The average IQ score for groups A_1 and A_2 was 4.46 ± 0.59 and 4.45 ± 0.62, respectively (Figures 3-5). There were no significant differences in IQ scores among the

Table 3 Computed tomography values and objective image quality scores for the aortic roots and proximal coronary vessels

Group, *n*	Aortic root, HU			Noise		
A_1, *n* = 82	512.18 ± 108.22	477.20 ± 117.93	485.88 ± 4100.40	15.52 ± 4.73	66.00 ± 25.30	41.32 ± 16.13
A_2, *n* = 39	601.92 ± 125.34	534.67 ± 117.33	546.99 ± 109.30	19.29 ± 6.26	54.28 ± 17.72	38.45 ± 12.06
P value	0.07	0.32	0.37	0.00	0.00	0.00

HU: Hounsfield unit.

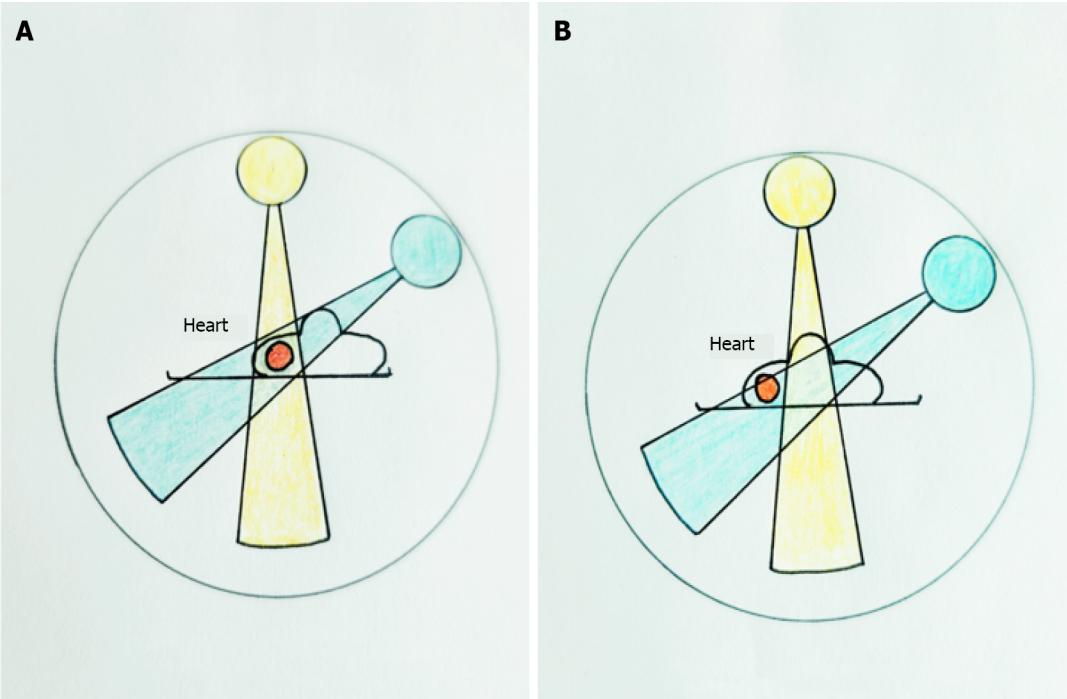

DOI: 10.4329/wjr.v15.i2.32 **Copyright** ©The Author(s) 2023.

Figure 1 For group A_1, the isocentric scan was performed with the patient in supine position and their body shifted to the right. A: Conventional position; B: Isocentric scanning.

two groups (*P* equal to 0.08-0.31). According to the observers, the subjective IQ values of the two groups were very high (intraclass correlation coefficients equal to 0.71-0.90; Tables 3 and 4).

DISCUSSION

In the present study, the multiple dose reduction scan techniques significantly decreased the ED during the CCTA of patients under clinical diagnosis situations. The radiation dose for the group with multiple dose reduction was approximately 33.63% (1.13 ± 0.35/3.36 ± 1.30) of the dose associated with the conventional method, and the proportion of IQ that met the needs for the clinical diagnosis was > 99% (images with IQ scores of ≥ 3). There was no difference in subjective IQ when compared to conventional coronary CT scans.

Previous studies have only employed lower tube voltages, smart milliampere[1,7,14], or merely a narrow acquisition window for dose reduction techniques in CCTA[16,17]. To our knowledge, the present study was the first in the English literature to combine multiple technologies (narrow acquisition window, tube voltage of 80 kV, smart milliampere, and isocentric scanning) to reduce the CCTA radiation dose. The ED was significantly higher in the conventional group when compared to the multi-modality group ($P < 0.05$). A previous study performed a low-dose CCTA with the a CT scanner by Canon with 640 slices on patients whose heart rate was less than 70 beats/min and reported the mean ED as 2.67 ± 0.5 mSv[14]. Similar to this, using the same signal equipment (Aquilion ONE Genesis, Canon Medical Systems), Di Cesare *et al*[18] and Li *et al*[7] determined that ED medians were 2.80 ± 0.57 and 3.36 ± 2.35 mSv, respectively. During the present study, the value of the latter was the same as that of the conventional group. Although multi-modality technology was used to reduce the radiation dose

Table 4 Subjective image quality scores and the number of score segments in the two groups

Group	All segments	5	4	3	2	1	Average IQ score
A_1	1085	420 (38.71%)	611 (56.48%)	45 (4.15%)	6 (0.55%)	1 (0.09%)	4.46 ± 0.59
A_2	518	258 (49.81%)	232 (44.79%)	19 (3.67%)	8 (1.54%)	1 (0.19%)	4.45 ± 0.62
P value							0.12

IQ: Image quality.

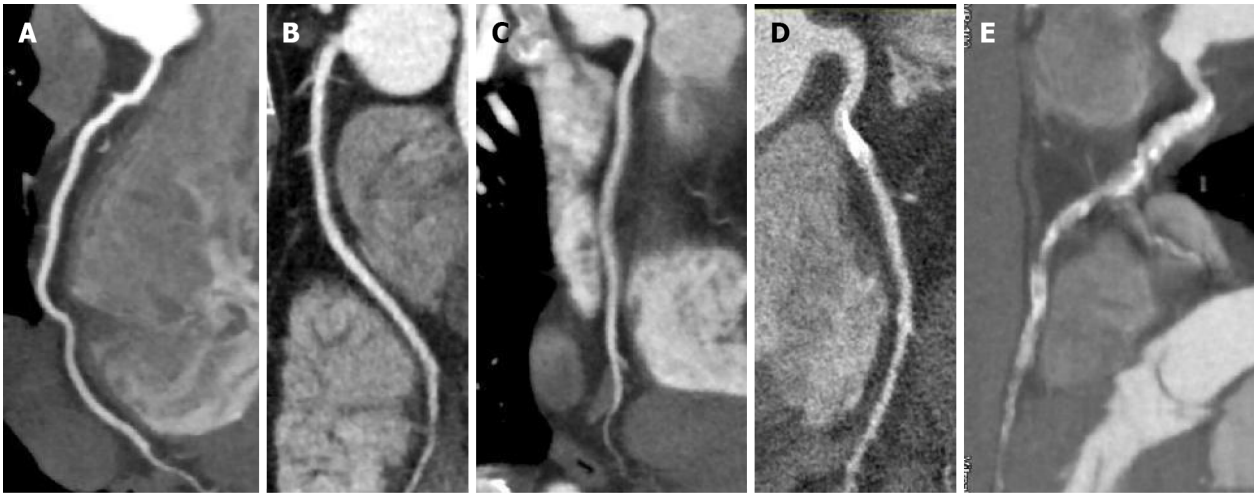

DOI: 10.4329/wjr.v15.i2.32

Figure 2 Subjective imaging quality scores. A: Excellent imaging quality (IQ) (score = 5) with sharp, smooth contours of the vascular wall and no streaking or radiating artifacts; B: Good IQ (score = 4) with slight irregularities on the contour and few streaks or radiating artifacts; C: Fair IQ (score = 3) with blurred and irregular contours of the vascular wall and numerous streaks or radiating artifacts; D: Poor IQ (score = 2) with deformation of the vascular wall and various artifacts; E: Very poor IQ (score = 1) with obvious deformation of the vascular wall and extensive artifacts. Images with IQ scores within 3-5 satisfy the requirements for the diagnostic assessment.

of CCTA, there were no significant differences in subjective IQ scores (P = 0.12).

The present study revealed that the radiation dose of CCTA significantly decreased after the application of multiple dose reduction scan techniques. The radiation dose in group A_1 was approximately 33.63% (1.13 ± 0.35/3.36 ± 1.30) in comparison with the traditional method. Low-dose CCTA has been shown to significantly reduce ED in some studies using dual source CTs (Siemens Healthcare)[7,14], GE gem energy spectrum CTs (GE Medical Systems)[8], as well as Philips Brilliance 256-slice iCTs (Philips Medical Systems)[4], with a tube voltage of 80 kV. The current research was the first to report the use of a low-dose CCTA at an 80 kV tube voltage utilizing a Canon CT system. A craniocaudal coverage of 16 cm was achieved, exceeding the length of the median scan employed in clinical practice. Furthermore, the tube generally rotates 360°, allowing it to be sufficient for cardiac scanning. Li *et al*[7] and Khosa *et al*[17] performed CCTA using the Canon 320-row dynamic CT system (Aquilion ONE, Toshiba Medical Systems; the present study used the same signal equipment), with a tube voltage of 120 kV. Both studies used the following parameters: RR interval, 66%-80%; BMI, 28 kg/m^2; and heart rate, < 70 bpm. Furthermore, the present study employed 1.54 mSv, while the study conducted by Khosa *et al* [17] employed 633 mSv. According to some studies, radiation doses can reach 1.76 ± 0.43-2.72 ± 0.50 mSv when CCTA is used with an 80 kV tube voltage[7,13] when compared to the doses in the present study, and the ED was high.

A positive correlation exists between the intensity of X-rays and the square of tube voltage and current. In contrast to lowering tube current, reducing tube voltage substantially reduces radiation dose. In previous research, low tube voltage was found to reduce radiation dosage. However, this has the disadvantage of increasing picture noise and lowering CNR, which limits the reduction of the radiation dose[17-19]. Adaptive Iterative Dose Reduction Using Three Dimensional Processing was used in those studies to reconstruct the image, and the results were compared using conventional methods. This approach effectively improved the IQ and reduced the radiation dose in scans for different areas[17-19]. In another study, the use of Adaptive Iterative Dose Reduction Using Three Dimensional Processing and ultra-low-dose CT has been shown to significantly increase IQ[20].

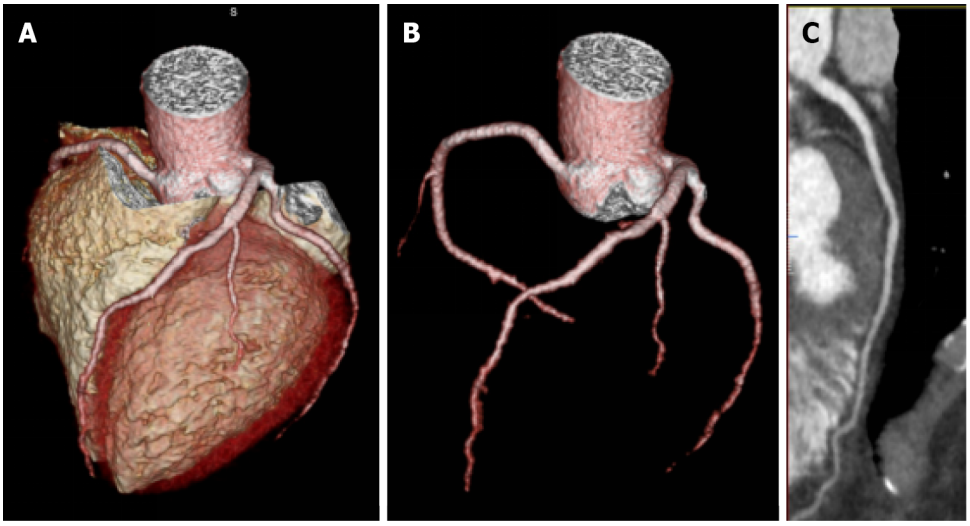

DOI: 10.4329/wjr.v15.i2.32 **Copyright** ©The Author(s) 2023.

Figure 3 A 69-year-old female patient in group A_1. For the multislice computed tomographic angiography, the image quality score was 5 (excellent) for left anterior descending artery segments 5-8. A and B: Volume rendering; C: Curved planar reformation. Body mass index: 26.40; Effective dose: 1.18 mSv; Noise: 18.80; Signal-to-noise ratio: 52.68; Contrast signal-to-noise ratio: 42.89.

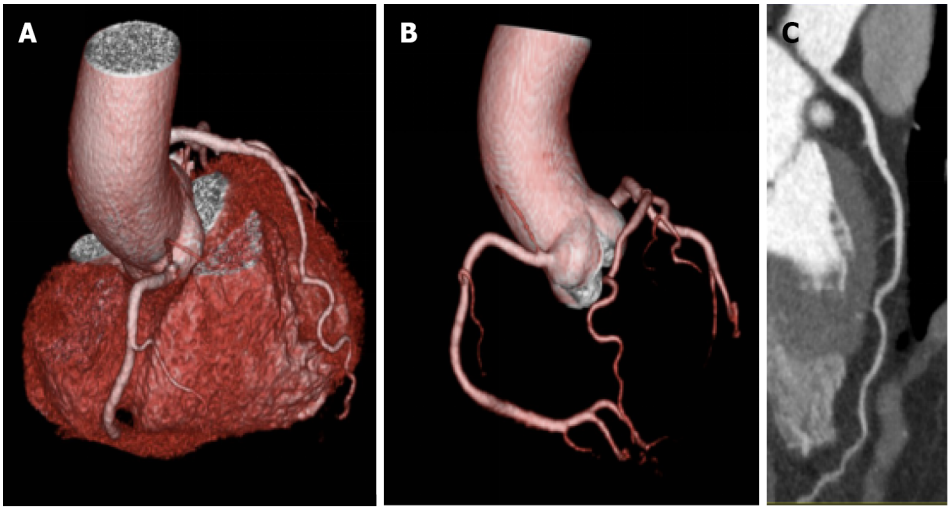

DOI: 10.4329/wjr.v15.i2.32 **Copyright** ©The Author(s) 2023.

Figure 4 A 64-year-old female patient in group A_1. For the multislice computed tomographic angiography, the image quality score was 5 (excellent) for left anterior descending artery segments 5-8. A and B: Volume rendering; C: Curved planar reformation. Body mass index: 26.40; Effective dose: 1.83 mSv; Noise: 22.50; Signal-to-noise ratio: 43.90; Contrast signal-to-noise ratio: 30.40.

Computed tomography angiography (CTA) is a non-invasive examination method and has the advantages of convenience, speed, safety, and reliability. This technique can clearly display the stenosis of the coronary lumen and plaque on the wall and determine whether the coronary artery has stenosis. Furthermore, its accuracy for CHD diagnosis is very high[17-19,21]. Digital subtraction angiography (DSA) is an invasive examination and is poorly accepted by patients. Coronary DSA can only determine vascular stenosis. Although coronary DSA is the gold standard for accurately determining vascular stenosis, it is an invasive examination with high radiation dose, high cost, and poor patient acceptance. A dose reduction on CTA examinations, such as the reduction of radiation exposure, could benefit patients with suspected CHD, who could not endure a DSA examination[22]. Our research group is performing further explorations on the effects of dose reduction techniques for patients who could not endure DSA examinations in order to increase its clinical practicability.

There are a few limitations to the current research. A minimum heart rate less than 70 beats/min was required for all patients, including those with low BMIs. A second drawback is that there was no correlation between the CCTA and DSA for the coronary artery, and the IQ was only rated subjectively for the coronary artery. A more in-depth investigation is required for individuals who are classified as obese according to their obesity grade (grade 1, BMI = 30-37.5 kg/m^2 and grade 3, BMI ≥ 37.5 kg/m^2).

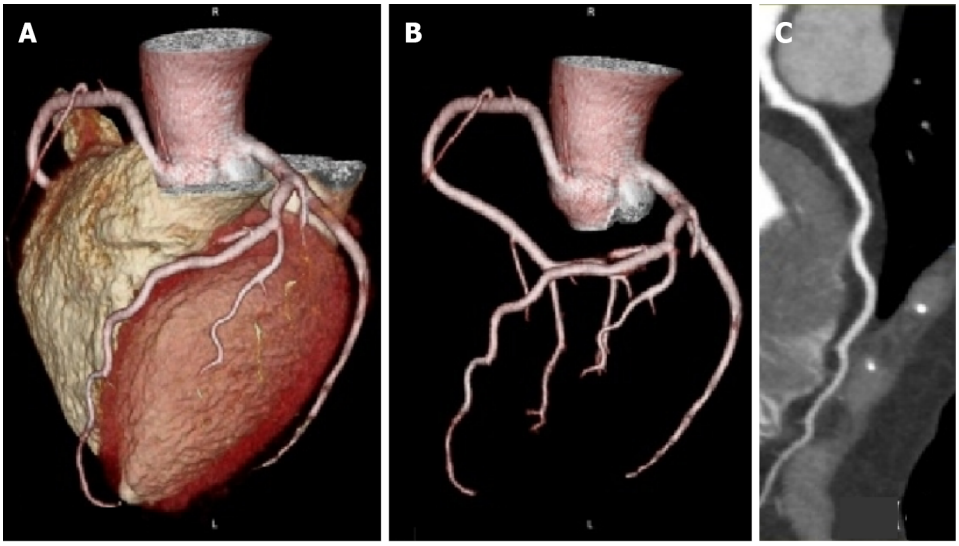

DOI: 10.4329/wjr.v15.i2.32

Figure 5 A 68-year-old female patient in group A_2. For the multislice computed tomographic angiography, the image quality score was 5 (excellent) for left anterior descending artery segments 5-8. A and B: Volume rendering; C: Curved planar reformation. Body mass index: 22.38; Effective dose: 3.33 mSv; Noise: 13.10; Signal-to-noise ratio: 74.69; Contrast signal-to-noise ratio: 58.85.

CONCLUSION

Multiple dose reduction scan techniques can significantly reduce the radiation dose under conditions that meet the requirements for clinical diagnosis.

ARTICLE HIGHLIGHTS

Research background

Coronary computed tomography angiography (CCTA) is considered to be an ideal non-invasive test for coronary heart disease (CHD). Nevertheless, as more people become aware of the dangers associated with radiation, the issue of computed tomography radiation has emerged as a major concern.

Research motivation

The present study aimed to explore the value of multiple dose reduction techniques on CCTA.

Research objectives

A consecutive sample of individuals with clinically suspected CHD was screened for inclusion in the current research. The inclusion criteria were: ≥ 18-years-old; heart rate less than 70 beats/min; and body mass index of 18.0 to 29.9 kg/m^2. Patients having pacemakers, significant respiratory artifacts, metallic implants located within the scanning range, an allergy to contrast agents or Betaloc, or patients who had undergone cardiac surgery or had a history of cardiac tumors were not eligible for treatment.

Research methods

Consecutive normal and overweight patients were prospectively divided into two groups: Group A_1, patients who received multiple dose reduction scans (n = 82); and group A_2, patients who received conventional scans (n = 39). The scan parameters for group A_1 consisted of the following: An isocentric scan, a tube voltage of 80 kV, and an 80% smart milliampere for tube current control. The scan parameters for group A_2 were as follows: Normal position, tube voltage = 100 kV, and smart milliampere.

Research results

The average effective doses (EDs) for groups A_1 and A_2 were 1.13 ± 0.35 and 3.36 ± 1.30 mSv, respectively. A statistically significant difference was found between the two groups in terms of ED (P < 0.01). The signal-to-noise ratio as well as contrast signal-to-noise ratio of group A2 were significantly higher than those of group A1, in addition to having less noise. Moreover, the subjective image quality (IQ) scores were excellent in both groups, and the subjective IQ scores of the two groups did not differ significantly (P = 0.12).

Research conclusions

Multiple dose reduction scan techniques can significantly decrease the ED of patients receiving CCTA examinations for clinical diagnosis.

Research perspectives

This study supports the application of the multiple dose reduction scan techniques in patients receiving CCTA.

FOOTNOTES

Author contributions: Hu XL and Huang PK were involved in drafting the manuscript; Zhang M and Huang PK were involved in acquisition of data; Chen J prepared the figures; Xiao MQ reviewed and revised the manuscript; All authors have read and approved the final manuscript.

Supported by Zhuhai Medical Research Fund, No. ZH3310200001PJL.

Institutional review board statement: This study was approved by the institutional review board of Guangdong Provincial Hospital of Traditional Chinese Medicine, No. BF2020-229-01.

Informed consent statement: All patients provided written consent, and written informed consent was obtained from each patient or the patient's family before performing the computed tomography scan. This study was conducted in accordance with the Declaration of Helsinki.

Conflict-of-interest statement: All the authors report no relevant conflicts of interest for this article.

Data sharing statement: The datasets used or analyzed during the current study are available from the corresponding author on reasonable request.

CONSORT 2010 statement: The authors have read the CONSORT 2010 Statement, and the manuscript was prepared and revised according to the CONSORT 2010 Statement.

Country/Territory of origin: China

ORCID number: Xiao-Lu Hu 0000-0003-4638-0646; Pei-Kai Huang 0000-0003-3463-5154; Jun Chen 0000-0002-1936-9954; Meng-Qiang Xiao 0000-0001-6970-6405.

S-Editor: Fan JR
L-Editor: Filipodia
P-Editor: Fan JR

REFERENCES

1 **Jia CF**, Zhong J, Meng XY, Sun XX, Yang ZQ, Zou YJ, Wang XY, Pan S, Yin D, Wang ZQ. Image quality and diagnostic value of ultra low-voltage, ultra low-contrast coronary CT angiography. *Eur Radiol* 2019; **29**: 3678-3685 [PMID: 30888481 DOI: 10.1007/s00330-019-06111-0]

2 **Serruys PW**, Hara H, Garg S, Kawashima H, Nørgaard BL, Dweck MR, Bax JJ, Knuuti J, Nieman K, Leipsic JA, Mushtaq S, Andreini D, Onuma Y. Coronary Computed Tomographic Angiography for Complete Assessment of Coronary Artery Disease: JACC State-of-the-Art Review. *J Am Coll Cardiol* 2021; **78**: 713-736 [PMID: 34384554 DOI: 10.1016/j.jacc.2021.06.019]

3 **Aghayev A**, Murphy DJ, Keraliya AR, Steigner ML. Recent developments in the use of computed tomography scanners in coronary artery imaging. *Expert Rev Med Devices* 2016; **13**: 545-553 [PMID: 27140944 DOI: 10.1080/17434440.2016.1184968]

4 **Tang S**, Zhang G, Chen Z, Liu X, He L. Application of prospective ECG-gated multiphase scanning for coronary CT in children with different heart rates. *Jpn J Radiol* 2021; **39**: 946-955 [PMID: 34046853 DOI: 10.1007/s11604-021-01133-5]

5 **Apfaltrer G**, Albrecht MH, Schoepf UJ, Duguay TM, De Cecco CN, Nance JW, De Santis D, Apfaltrer P, Eid MH, Eason CD, Thompson ZM, Bauer MJ, Varga-Szemes A, Jacobs BE, Sorantin E, Tesche C. High-pitch low-voltage CT coronary artery calcium scoring with tin filtration: accuracy and radiation dose reduction. *Eur Radiol* 2018; **28**: 3097-3104 [PMID: 29404770 DOI: 10.1007/s00330-017-5249-2]

6 **Zhang W**, Ba Z, Wang Z, Lv H, Zhao J, Zhang Y, Zhang F, Song L. Diagnostic performance of low-radiation-dose and low-contrast-dose (double low-dose) coronary CT angiography for coronary artery stenosis. *Medicine (Baltimore)* 2018; **97**: e11798 [PMID: 30142766 DOI: 10.1097/MD.0000000000011798]

7 **Li RF**, Hou CL, Zhou H, Dai YS, Jin LQ, Xi Q, Zhang JH. Comparison on radiation effective dose and image quality of right coronary artery on prospective ECG-gated method between 320 row CT and 2nd generation (128-slice) dual source CT. *J Appl Clin Med Phys* 2020; **21**: 256-262 [PMID: 32510768 DOI: 10.1002/acm2.12911]

8 **Liu K**, Diao K, Hu S, Xu X, Zhang J, Peng W, Xia C, Zhang K, Li Y, Guo Y, He S, He Y, Li Z. Achieving Low Radiation Dose in "One-Stop" Myocardial Computed Tomography Perfusion Imaging in Coronary Artery Disease Using 16-cm Wide Detector CT. *Acad Radiol* 2020; **27**: 1531-1539 [PMID: 31859211 DOI: 10.1016/j.acra.2019.11.018]

9 **Ali I**, Ahmad S. Evaluation of the effects of sagging shifts on isocenter accuracy and image quality of cone-beam CT from kV on-board imagers. *J Appl Clin Med Phys* 2009; **10**: 180-194 [PMID: 19692976 DOI: 10.1120/jacmp.v10i3.2930]

10 **Chow JC**. Cone-beam CT dosimetry for the positional variation in isocenter: a Monte Carlo study. *Med Phys* 2009; **36**: 3512-3520 [PMID: 19746785 DOI: 10.1118/1.3166934]

11 **Dane B**, O'Donnell T, Liu S, Vega E, Mohammed S, Singh V, Kapoor A, Megibow A. Radiation dose reduction, improved isocenter accuracy and CT scan time savings with automatic patient positioning by a 3D camera. *Eur J Radiol* 2021; **136**: 109537 [PMID: 33454459 DOI: 10.1016/j.ejrad.2021.109537]

12 **Olden KL**, Kavanagh RG, James K, Twomey M, Moloney F, Moore N, Carey K, Murphy KP, Grey TM, Nicholson P, Chopra R, Maher MM, O'Connor OJ. Assessment of isocenter alignment during CT colonography: Implications for clinical practice. *Radiography (Lond)* 2018; **24**: 334-339 [PMID: 30292502 DOI: 10.1016/j.radi.2018.04.003]

13 **Khan AR**, Awan FR, Najam SS, Islam M, Siddique T, Zain M. Elevated serum level of human alkaline phosphatase in obesity. *J Pak Med Assoc* 2015; **65**: 1182-1185 [PMID: 26564289]

14 **Cao JX**, Wang YM, Lu JG, Zhang Y, Wang P, Yang C. Radiation and contrast agent doses reductions by using 80-kV tube voltage in coronary computed tomographic angiography: a comparative study. *Eur J Radiol* 2014; **83**: 309-314 [PMID: 24315475 DOI: 10.1016/j.ejrad.2013.06.032]

15 **Nakanishi R**, Sankaran S, Grady L, Malpeso J, Yousfi R, Osawa K, Ceponiene I, Nazarat N, Rahmani S, Kissel K, Jayawardena E, Dailing C, Zarins C, Koo BK, Min JK, Taylor CA, Budoff MJ. Automated estimation of image quality for coronary computed tomographic angiography using machine learning. *Eur Radiol* 2018; **28**: 4018-4026 [PMID: 29572635 DOI: 10.1007/s00330-018-5348-8]

16 **Smit EB**, Bouwstra H, Roorda LD, van der Wouden JHC, Wattel ELM, Hertogh CMPM, Terwee CB. A Patient-Reported Outcomes Measurement Information System Short Form for Measuring Physical Function During Geriatric Rehabilitation: Test-Retest Reliability, Construct Validity, Responsiveness, and Interpretability. *J Am Med Dir Assoc* 2021; **22**: 1627-1632.e1 [PMID: 33640312 DOI: 10.1016/j.jamda.2021.01.079]

17 **Khosa F**, Khan A, Nasir K, Shuaib W, Budoff M, Blankstein R, Clouse ME. Influence of image acquisition on radiation dose and image quality: full *vs* narrow phase window acquisition using 320 MDCT. *ScientificWorldJournal* 2013; **2013**: 731590 [PMID: 24453899 DOI: 10.1155/2013/731590]

18 **Di Cesare E**, Gennarelli A, Di Sibio A, Felli V, Splendiani A, Gravina GL, Masciocchi C. Image quality and radiation dose of single heartbeat 640-slice coronary CT angiography: a comparison between patients with chronic atrial fibrillation and subjects in normal sinus rhythm by propensity analysis. *Eur J Radiol* 2015; **84**: 631-636 [PMID: 25617080 DOI: 10.1016/j.ejrad.2014.11.035]

19 **Liu S**, Fu Q, Yu H, Zhang C, Yang Q, Hu Y, Xu W. Evaluate of the effect of low tube voltage on the radiation dosage using 640-slice coronary CT angiography. *J Xray Sci Technol* 2018; **26**: 463-471 [PMID: 29562576 DOI: 10.3233/XST-17332]

20 **Xiao M**, Zhang M, Lei M, Hu X, Wang Q, Chen Y, Ye J, Xu R, Chen J. Application of ultra-low-dose CT in 3D printing of distal radial fractures. *Eur J Radiol* 2021; **135**: 109488 [PMID: 33385624 DOI: 10.1016/j.ejrad.2020.109488]

21 **Di Cesare E**, Gennarelli A, Di Sibio A, Felli V, Perri M, Splendiani A, Gravina GL, Barile A, Masciocchi C. 320-row coronary computed tomography angiography (CCTA) with automatic exposure control (AEC): effect of 100 kV *vs* 120 kV on image quality and dose exposure. *Radiol Med* 2016; **121**: 618-625 [PMID: 27169907 DOI: 10.1007/s11547-016-0643-4]

22 **Guo W**, Liu X, Gao Z, Pirbhulal S, Huang W, Lin WH, Zhang H, Tan N, Zhang YT. Quantification of three-dimensional computed tomography angiography for evaluating coronary luminal stenosis using digital subtraction angiography as the standard of reference. *Biomed Eng Online* 2015; **14**: 50 [PMID: 26024658 DOI: 10.1186/s12938-015-0048-y]

World Journal of Radiology

Submit a Manuscript: https://www.f6publishing.com

World J Radiol 2023 February 28; 15(2): 42-55

DOI: 10.4329/wjr.v15.i2.42

ISSN 1949-8470 (online)

SYSTEMATIC REVIEWS

Imaging of paraduodenal pancreatitis: A systematic review

Matteo Bonatti, Nicolò De Pretis, Giulia A Zamboni, Alessandro Brillo, Stefano Francesco Crinò, Riccardo Valletta, Fabio Lombardo, Giancarlo Mansueto, Luca Frulloni

Specialty type: Radiology, nuclear medicine and medical imaging

Provenance and peer review: Invited article; Externally peer reviewed.

Peer-review model: Single blind

Peer-review report's scientific quality classification
Grade A (Excellent): 0
Grade B (Very good): 0
Grade C (Good): C
Grade D (Fair): D, D
Grade E (Poor): 0

P-Reviewer: Kaneko J, Japan; Tellez-Avila F, United States

Received: September 28, 2022
Peer-review started: September 28, 2022
First decision: October 17, 2022
Revised: October 24, 2022
Accepted: December 6, 2022
Article in press: December 6, 2022
Published online: February 28, 2023

Matteo Bonatti, Riccardo Valletta, Department of Radiology, Ospedale Centrale di Bolzano, Bolzano 39100, Italy

Nicolò De Pretis, Alessandro Brillo, Luca Frulloni, Gastroenterology and Digestive Endoscopy Unit, The Pancreas Institute, G.B. Rossi University Hospital of Verona, Verona 37134, Italy

Giulia A Zamboni, Giancarlo Mansueto, Department of Diagnostics and Public Health, Radiology Section, Policlinico GB Rossi, University of Verona, Verona 37134, Verona, Italy

Stefano Francesco Crinò, Department of Medicine, University of Verona, Verona 37134, Italy

Fabio Lombardo, Department of Radiology, IRCCS Sacro Cuore Don Calabria Hospital, Negrar 37024, Italy

Corresponding author: Matteo Bonatti, MD, Adjunct Professor, Doctor, Department of Radiology, Ospedale Centrale di Bolzano, Via Boehler 5, 39100 Bolzano, Italy. matteo.bonatti@sabes.it

Abstract

BACKGROUND

Paraduodenal pancreatitis (PP) represents a diagnostic challenge, especially in non-referral centers, given its potential imaging overlap with pancreatic cancer. There are two main histological variants of PP, the cystic and the solid, with slightly different imaging appearances. Moreover, imaging findings in PP may change over time because of disease progression and/or as an effect of its risk factors exposition, namely alcohol intake and smoking.

AIM

To describe multimodality imaging findings in patients affected by PP to help clinicians in the differential diagnosis with pancreatic cancer.

METHODS

The systematic review was conducted according to the Preferred Reporting Items for Systematic reviews and Meta-analyses 2009 guidelines. A Literature search was performed on PubMed, Embase and Cochrane Library using (groove pancreatitis [Title/Abstract]) OR (PP [Title/Abstract]) as key words. A total of 593 articles were considered for inclusion. After eliminating duplicates, and title and abstract screening, 53 full-text articles were assessed for eligibility. Eligibility criteria were: Original studies including 8 or more patients, fully written in English, describing imaging findings in PP, with pathological confirmation or

clinical-radiological follow-up as the gold standard. Finally, 14 studies were included in our systematic review.

RESULTS

Computed tomography (CT) findings were described in 292 patients, magnetic resonance imaging (MRI) findings in 231 and endoscopic ultrasound (EUS) findings in 115. Duodenal wall thickening was observed in 88.8% of the cases: Detection rate was 96.5% at EUS, 91.0% at MRI and 84.1% at CT. Second duodenal portion increased enhancement was recognizable in 76.3% of the cases: Detection rate was 84.4% at MRI and 72.1% at CT. Cysts within the duodenal wall were detected in 82.6% of the cases: Detection rate was 94.4% at EUS, 81.9% at MRI and 75.7% at CT. A solid mass in the groove region was described in 40.9% of the cases; in 78.3% of the cases, it showed patchy enhancement in the portal venous phase, and in 100% appeared iso/hyperintense during delayed phase imaging. Only 3.6% of the lesions showed restricted diffusion. The prevalence of radiological signs of chronic obstructive pancreatitis, namely main pancreatic duct dilatation, pancreatic calcifications, and pancreatic cysts, was extremely variable in the different articles.

CONCLUSION

PP has peculiar imaging findings. MRI is the best radiological imaging modality for diagnosing PP, but EUS is more accurate than MRI in depicting duodenal wall alterations.

Key Words: Pancreatitis; Paraduodenal pancreatitis; Diagnostic imaging; Computed tomography; Magnetic resonance imaging; Endoscopic ultrasound

Core Tip: Paraduodenal pancreatitis (PP) represents a diagnostic challenge, especially in non-referral centers, given its potential imaging overlap with neoplastic processes, namely pancreatic and duodenal carcinoma. Numerous articles show imaging features of PP, but most of them are represented by case reports or reviews with poor scientific background. This systematic review describes the multimodality imaging features (computed tomography, magnetic resonance imaging and endoscopic ultrasound) of PP according to original research articles with pathologic samples and or clinical-radiological follow-up as the gold standard.

Citation: Bonatti M, De Pretis N, Zamboni GA, Brillo A, Crinò SF, Valletta R, Lombardo F, Mansueto G, Frulloni L. Imaging of paraduodenal pancreatitis: A systematic review. *World J Radiol* 2023; 15(2): 42-55
URL: https://www.wjgnet.com/1949-8470/full/v15/i2/42.htm
DOI: https://dx.doi.org/10.4329/wjr.v15.i2.42

INTRODUCTION

Paraduodenal pancreatitis (PP), also known as groove pancreatitis, is a peculiar form of chronic pancreatitis characterized by an inflammatory mass-forming involvement of the duodenal wall in the so-called groove area, located between the head of the pancreas, the duodenum, and the common bile duct[1]. The inflammatory process may lead to a solid thickening of the duodenal wall and/or to the development of cystic changes centered in the groove area. PP has been subdivided into cystic or solid type, based on the presence or absence of cysts in the groove area at imaging or pathology. According to a large Italian study, two thirds of patients present the cystic type of PP and one third the solid one[2]; similar data were reported on a more limited series from India[3]. The inflammatory process, arising from the groove area, might also extend to the whole pancreas secondary to the compression and obstruction of the main pancreatic duct by the inflamed and thickened groove area, leading to obstructive chronic pancreatitis. No definitive epidemiological data have been published, but PP is a rare disease considering that in an observational study including 893 patients with chronic pancreatitis, PP prevalence was 6%[4]. On the other hand, a German study published in 2014 reported 3.5% of PP on 373 consecutive pancreatic resections in a single center[5].

Adsay *et al*[1] described the typical histological features of PP, namely dilated ducts in the duodenal wall with pseudocystic changes and granulation tissue, Brunner's gland hyperplasia, dense myoid stromal proliferation and fibrosis of the pancreas and of the surrounding soft tissue of the groove area [1].

As reported by many previously published papers, patients suffering from PP are typically middle-aged men, heavy smokers, and drinkers[2-4,6-14]. Acute pancreatitis and abdominal pain have been described as the most frequent presenting symptoms, followed by symptoms related to duodenal obstruction (vomiting and weight loss) and to common bile duct obstruction (jaundice)[2,9-11]. Symptoms related to pancreatic insufficiency (diabetes and steatorrhea) are less frequent and generally reported in patients with advanced disease.

PP diagnosis may be challenging since patients often present with symptoms mimicking pancreatic cancer, such as abdominal pain, vomiting, weight loss or jaundice, and, especially in the solid type, also at imaging the differential diagnosis with pancreatic cancer can be extremely difficult. Therefore, a significant proportion of patients (reported between 5% and 21%, even in referral centers) undergo demolitive pancreatic surgery because of misdiagnosis or malignancy suspicion[2,6,15,16].

Many different therapeutic strategies have been proposed for symptoms' management in PP and, nowadays, no definitive data have been published about the best choice between medical treatment and endoscopic or surgical interventions. A step-up approach should probably be considered, starting with medical treatment based on pain control, alcohol consumption cessation, and smoke cessation. Endoscopic treatment might be considered in the case of bile duct stenosis and surgery should be reserved for patients with intractable pain, duodenal obstruction, or recurrent bile duct obstruction and cholangitis.

Despite the rarity of the disease, a precise radiological and clinical diagnosis is crucial for patients' management and a multidisciplinary approach is needed to reduce the risk of misdiagnosis and of inappropriate surgical resections. Therefore, the aim of our study was to conduct a systematic literature review to show the multimodality imaging appearance of PP and to assess imaging performance in the differential diagnosis between PP and pancreatic cancer.

MATERIALS AND METHODS

Studies selection

The study was conducted according to the Preferred Reporting Items for Systematic reviews and Meta-analyses (PRISMA) guidelines. We performed a database search on PubMed, Embase and Cochrane Library, looking for articles published from January 1990 to July 2022. The following string was used: (Groove pancreatitis [Title/Abstract]) OR (PP [Title/Abstract]). A total of 593 papers were identified and considered for inclusion. After eliminating duplicates, and title and abstract screening, 53 full-text articles were assessed for eligibility by two radiologists independently. Discrepancies were solved by consensus, which was necessary in 2 cases. Eligibility criteria were original studies including 8 or more patients, written in English, describing imaging findings in PP, with pathological confirmation or clinical-radiological follow-up as the gold standard (Figure 1). Finally, 14 studies were included in our systematic review[2,3,7,9,11,12,15-22].

Data extraction

Study characteristics, including publication date, journal type, inclusion period, aim of the study, study design, characteristics of the patients considered for inclusion, number of patients with PP included, and study limitations were extracted from the included studies (Table 1). The presence of potential bias was evaluated by two Authors in consensus using the Newcastle-Ottawa Quality Assessment Scale for Cohort Studies (https://www.ohri.ca/programs/clinical_epidemiology/oxford.asp) (Table 2). The maximum number of points given to each item was 4, 2 and 3, with a total maximum number of 9 points.

The following data were extracted from the included studies: Number of patients examined with the different imaging modalities [computed tomography (CT), magnetic resonance imaging (MRI), ultrasound (US), and endoscopic ultrasound (EUS)], PP variant (cystic/solid), lesions' size (mean maximum and minimum diameter), presence of duodenal wall thickening (yes/no), duodenal wall thickening distribution (eccentric/circumferential), presence of second duodenal portion increased wall enhancement (yes/no), presence (yes/no) number (single/multiple) and size (mm) of duodenal wall cysts, presence of a discrete pancreatic mass (yes/no), lesion's signal intensity on T2-weighted images, on T1-weighted images, on high b value diffusion-weighted images and on apparent diffusion coefficient (ADC) map (hypo-/iso-/hyper-intense in comparison to "normal" pancreas), enhancement on arterial, portal venous and delayed phase images (hypo-/iso-/hyper-intense/dense in comparison to "normal" pancreas), enhancement pattern in portal venous phase (hypo/patchy/rim), presence of pancreatic cysts (yes/no), presence of main pancreatic duct dilatation (yes/no), presence of pancreatic calcifications (yes/no), presence of biliary duct dilatation (yes/no), presence of portal vein stenosis (yes/no), presence of gastroduodenal artery displacement (yes/no), presence of peripancreatic fat stranding (yes/no), presence of peripancreatic enlarged lymph nodes (yes/no). The above-mentioned variables were not considered in every study (Tables 3 and 4). The absolute number of patients for which the variable was evaluated is reported in the text as (n = #).

Table 1 Characteristics of the included studies

Ref.	Year	Journal type	Aim	Inclusion period	Study design	Patients considered for inclusion	Paraduodenal pancreatitis patients included	Limitations
Ishigami *et al* [17]	2010	Radiological	Differential diagnosis cancer *vs* paraduodenal pancreatitis	2001-2008	Retrospective, single center	Institutional database search using "groove pancreatitis or groove pancreatic carcinoma" (*n* = 22)	15	Small population, no clear distinction between computed tomography and magnetic resonance imaging findings
Kalb *et al*[18]	2013	Radiological	Differential diagnosis cancer *vs* paraduodenal pancreatitis	2007-2010	Retrospective, single center	Institutional database search using "Whipple and/or pancreatectomy" and diagnosis of cancer or paraduodenal pancreatitis (*n* = 47)	17	Surgically resected patients only, small population
Zaheer *et al* [19]	2014	Radiological	Findings description	2002-2013	Retrospective, single center	Patients undergoing pancreaticoduodenectomy and histological paraduodenal pancreatitis diagnosis (*n* = 12)	12	Surgically resected patients only, small population
Arvanitakis *et al*[11]	2014	Gastroenterological	Endoscopic and medical management	1995-2010	Retrospective, single center	Institutional database search using "paraduodenal pancreatitis" (*n* = 51)	51	Poor imaging findings description based on radiological reports
Wagner *et al* [20]	2015	Radiological	Findings description	"14 yr"	Retrospective, single center	Patients with cystic dystrophy in heterotopic pancreas diagnosis at endoscopic ultrasound (*n* = 138)	76	Only cystic variant of paraduodenal pancreatitis included
Arora *et al*[3]	2015	Radiological	Findings description	2010-2014	Retrospective, single center	Patients treated for paraduodenal pancreatitis at gastroenterology or surgical units (*n* = 33)	33	Poor imaging findings description based on radiological reports, no clear distinction between computed tomography and magnetic resonance imaging findings
Shin *et al*[21]	2016	Radiological	Differential diagnosis cancer *vs* paraduodenal pancreatitis	2005-2011	Retrospective, 2 centers	Multidetector computed tomography for pancreas protocols (*n* = 2561) with groove mass	8	Surgically resected patients only, small population
Boninsegna *et al*[22]	2017	Radiological	Differential diagnosis cancer *vs* paraduodenal pancreatitis	2012-2015	Retrospective, single center	Abdominal Magnetic Resonance Imaging with groove mass	28	None
de Pretis *et al* [2]	2017	Multidisciplinary	Clinical and morphological features	1994-2012	Retrospective, single center	Patients with diagnosis of paraduodenal pancreatitis (*n* = 120)	120	Poor imaging findings description based on radiological reports, no clear distinction between computed tomography and magnetic resonance imaging findings
Muraki *et al* [9]	2017	Surgical	Imaging and pathologic correlation	2004-2015	Retrospective, single center	All pancreatic resections	47	Surgically resected patients only, poor imaging findings description, no clear distinction between computed tomography and magnetic resonance imaging findings
Tarvainen *et al*[16]	2021	Multidisciplinary	Diagnosis, natural course and treatment	2005-2015	Retrospective, multicentric	Institutional database search using "groove and/or paraduodenal" (*n* = 192)	33	Poor imaging findings description, no clear distinction between computed tomography and magnetic resonance imaging findings
Ooka *et al*[7]	2021	Gastroenterological	Clinical management	2000-2014	Retrospective,	Institutional database search using "groove pancre-	48	No clear distinction between computed

					single center	atitis and/or paraduodenal pancreatitis" (n = 211)		tomography and magnetic resonance imaging findings
Değer *et al* [15]	2022	Surgical	Clinical features and outcome	2013-2019	Retrospective, single center	Institutional database search using "groove and/or paraduodenal" (n = 28)	25	Poor imaging findings description based on radiological reports, no clear distinction between computed tomography and magnetic resonance imaging findings
Kulkarni *et al* [12]	2022	Radiological	Findings description	2007-2020	Retrospective, single center	Patients with pancreatitis (n = 2120)	30	None

Diagnostic performance of imaging studies in the differential diagnosis between PP and pancreatic cancer was also assessed.

Statistical analysis

Absolute numbers and percentages were used to describe quantitative variables. For continuous data, mean values were calculated. Sensitivity, specificity, negative predictive value and positive predictive value in differentiating between PP and pancreatic cancer were reported, when available. P values <0.05 were considered statistically significant.

RESULTS

Included studies characteristics

All the included studies had a retrospective design and encompassed a total of 543 patients, 489 (90%) males and 54 (10%) females, with a mean age of 48 years. History of chronic alcohol abuse was reported in 87% of the cases (n = 524) and 78% of the patients were heavy smokers (n = 334). The included studies were published on radiological journals in 8/14 cases (n = 219), on multidisciplinary journals in 2/14 (n = 153), on gastroenterological journals in 2/14 (n = 99), and on surgical journals in 2/14 (n = 72).

Pathology was the gold standard in 9/14 studies (n = 261), pathology or clinical-radiological follow up in 3/14 (n = 183), follow-up alone in 2/14 (n = 99). Cross-sectional images were reviewed by one or two Radiologists in 10/14 studies (n = 314), whereas in 4/14 studies (n = 229) the described CT and MRI imaging findings were based on the original radiological reports.

Nine out of the 14 evaluated studies included imaging findings obtained from 2 or more imaging modalities, whereas 4 studies were based on CT images only and 3 on MRI only. In 7 of the included studies, it was not always possible to clearly understand if the described findings were derived from CT or MRI images. Therefore, CT findings were described for 292 patients, MRI findings for 231 and EUS findings for 115; US findings were not described in any of the included studies.

Duodenal findings

Duodenal wall thickening was described in 88.8% of the cases (n = 420); at EUS, duodenal thickening was recognizable in 96.5% of the cases (n = 115), at MRI in 91.0% (n = 78) and at CT in 84.1% (n = 227). The cutoff value for the duodenal wall thickening definition was reported in three studies[18,21,22] (n =

Table 2 Risk of bias assessment

Ref.	Representativeness of the exposed cohort	Selection of the non-exposed cohort	Ascertainment of exposure	Outcome of interest was not present at start of study	Comparability of cohorts	Assessment of outcome	Follow-up long enough	Adequacy of follow up	Total
Ishigami *et al*[17]	±	-	-	-	-	-	NA	NA	6
Kalb *et al* [18]	±	-	-	-	-	-	NA	NA	6
Zaheer *et al* [19]	±	NA	-	+	NA	-	NA	NA	2
Arvanitakis *et al*[11]	±	NA	±	+	NA	-	-	-	3
Wagner *et al*[20]	+	NA	±	-	NA	+	NA	NA	1
Arora *et al* [3]	±	NA	±	+	NA	-	-	-	3
Shin *et al* [21]	±	-	-	-	±	-	NA	NA	4
Boninsegna *et al*[22]	-	±	-	-	±	-	NA	NA	4
de Pretis *et al*[2]	-	NA	-	-	NA	-	-	-	6
Muraki *et al* [9]	-	-	-	-	-	-	NA	NA	7
Tarvainen *et al*[16]	±	±	-	-	-	-	-	-	6
Ooka *et al* [7]	-	-	-	-	-	-	-	-	9
Değer *et al* [15]	-	NA	-	-	NA	-	-	-	6
Kulkarni *et al*[12]	-	NA	-	-	NA	-	NA	NA	4

-: Low risk of bias; ±: Unknown risk of bias; +: High risk of bias; NA: Not appliable.

53) and was 3 mm in all of them. Mean maximum duodenal wall thickness was assessed in two studies [19,20] and was 19 mm (n = 88). Wall thickening distribution was evaluated in one study only[19] and was eccentric, involving the second duodenal portion medial wall, in 81.8% of the cases and concentric in 18.2% (n = 11). The second duodenal portion showed an increased enhancement in comparison to the adjacent intestinal walls in 76.3% of the cases (n = 93); second duodenal portion increased enhancement was recognizable in 84.4% of the cases at MRI (n = 32) and in 72.1% at CT (n = 61).

Cysts within the duodenal wall were detected in 82.6% of the cases (n = 419); duodenal wall cysts were recognizable in 94.4% of the cases at EUS (n = 108), in 81.9% of the cases at MRI (n = 138) and in 75.7% of the cases at CT (n = 173). Duodenal wall cysts were single in 65.8% of the cases and multiple in 34.2% (n = 149). Cyst size was evaluated in three studies[9,18,20]. Muraki *et al*[9] and Wagner *et al*[20] reported a mean maximum size of the cystic component of 13 mm (n = 123), whereas Kalb *et al*[18] reported cystic components diameters ranging from 6 to 27 mm (n = 17).

The cystic variant of PP was depicted in 72.0% of the cases and the solid variant in 28.0% (n = 543).

Groove region findings

A solid mass in the groove region was described in 40.9% of the cases (n = 88). Mean maximum diameter of the lesion was 38 mm (n = 75), whereas mean minimum diameter was 16 mm (n = 27). Lesions' signal intensity on T2-weighted images was evaluated in two articles[17,22] (n = 43): The solid lesion was iso-intense to "normal" pancreatic parenchyma in 48.8% of the cases, hyperintense in 30.2% and hypointense in 21.0%. Lesions' signal intensity on other imaging sequences was assessed only by Boninsegna *et al*[22] (n = 28): On T1-weighted images the lesion was hypointense in 64.3% of the cases

Table 3 Variables evaluated in the included studies

Ref.	Duodenal wall thickening	Thickening distribution	Duodenal wall enhancement	Duodenal wall cysts	Cysts number	Cysts size	Pancreatic mass	Signal intensity on T2-weighted images	Signal intensity on T1-weighted images, diffusion-weighted images, apparent diffusion coefficient map	Arterial phase enhancement	Portal venous phase enhancement
Ishigami *et al* [17]				+				+			
Kalb *et al*[18]	+		+	+		1					
Zaheer *et al* [19]	1, 2	1		1			1, 2			1	1
Arvanitakis *et al*[11]	2			+, 2	+, 2						
Wagner *et al* [20]	1, 2			+, 1, 2	1	1					
Arora *et al*[3]	+, 1		+, 1	+, 1							
Shin *et al*[21]	1										1
Boninsegna *et al*[22]	+							+	+	+	+
de Pretis *et al* [2]											
Muraki *et al* [9]						+					
Tarvainen *et al*[16]											
Ooka *et al*[7]	1						1				
Değer *et al* [15]	+, 1			+, 1			1				
Kulkarni *et al* [12]	1		1	1							

+: Described at MRI; 1: Described at CT; 2: Described at EUS; MRI: Magnetic resonance imaging; EUS: Endoscopic ultrasound; CT: Computed tomography.

and isointense in 35.7%, on high b-value diffusion-weighted images it was isointense in 71.4% of the cases and hypointense in 28.6%, whereas on ADC maps it was isointense in 71.4% of the cases, hyperintense in 25.0% and hypointense in 3.6%. During the arterial phase of the dynamic study, the lesion appeared hypovascular in 82.4% of the cases and isovascular in 17.6% (n = 34). During the portal

Table 4 Variables evaluated in the included studies

Ref.	Delayed enhancement	Enhancement pattern	Pancreatic cysts	Main pancreatic duct dilatation	Pancreatic calcifications	Biliary duct dilatation	Portal vein stenosis	Gastroduodenal artery displacement	Peripancreatic fat stranding	Peripancreatic lymph nodes
Ishigami *et al* [17]		+		+	1	+				
Kalb *et al*[18]			+	+		+	+			
Zaheer *et al* [19]			2	1	1	1			1	1
Arvanitakis *et al*[11]				+, 1	1	+, 1				
Wagner *et al* [20]				+, 1	1	+, 1			1	
Arora *et al*[3]			+, 1	+, 1	1	+, 1		+, 1		
Shin *et al*[21]		1	1	1	1	1		1		1
Boninsegna *et al*[22]	+		+	+		+				
de Pretis *et al* [2]					1					
Muraki *et al*[9]			+	+		+, 1				
Tarvainen *et al* [16]			+, 1	+, 1	1	+, 1				
Ooka *et al*[7]			1	1	1				1	
Değer *et al*[15]				+, 1						
Kulkarni *et al* [12]			1	1	1	1		1		

+: Described at MRI; 1: Described at CT; 2: Described at EUS; MRI: Magnetic resonance imaging; EUS: Endoscopic ultrasound; CT: Computed tomography.

venous phase, the lesion appeared isovascular in 47.6% of the cases, hypovascular in 42.9% and hypervascular in 9.5% (n = 42). Enhancement pattern during the portal venous phase was described as "patchy" in 78.3% of the cases, whereas no cases of ring enhancement were detected (n = 23). During the delayed phase, the lesion appeared hyperintense in 53.6% of the cases and isointense in 46.4% (n = 28).

Pancreatic findings

Main pancreatic duct dilatation was present in 56.5% of the cases (n = 499); in the single included studies, prevalence of main pancreatic duct dilatation ranged from 28.9%[16] to 95.5%[20]. Pancreatic

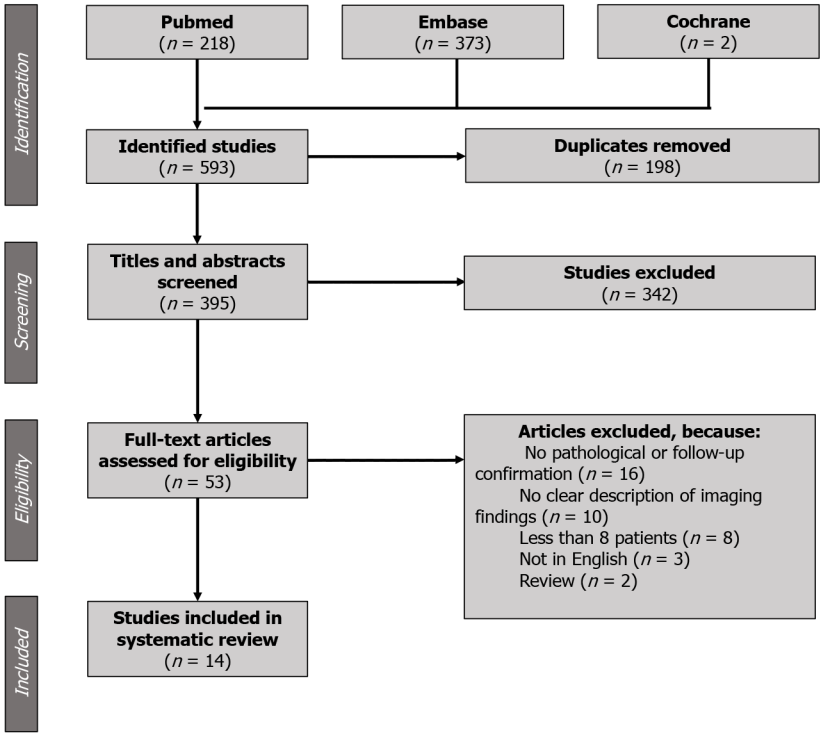

DOI: 10.4329/wjr.v15.i2.42

Figure 1 PRISMA flowchart showing studies inclusion and exclusion criteria.

cysts were detected in 64.5% of the cases (n = 269); pancreatic cysts detection rate was 80.3% at MRI (n = 122), 52.4% at CT (n = 147) and 42.9% (n = 7) at EUS. Pancreatic calcifications were present in 48.3% of the cases (n = 383); in the single included studies, prevalence of pancreatic calcifications ranged from 20%[7] to 100%[11]. Calcifications in the region of the minor papilla were recognizable in 43.4% of the cases (n = 76).

Alterations in the adjacent structures

Biliary duct dilatation was observed in 41.2% of the cases (n = 417), portal vein stenosis in 47.1% (n = 17) and gastroduodenal artery displacement in 64.3% (n = 84). Peripancreatic fat stranding was described in 88.1% of the cases (n = 134) and enlarged peripancreatic lymph nodes were appreciable in 65.0% (n = 20).

Differential diagnosis PP vs cancer

Four articles[17,18,21,22] explored imaging accuracy in the differential diagnosis between PP and pancreatic cancer, including a total of 68 patients with PP and 73 with pancreatic adenocarcinoma. Shin *et al*[21] showed that, at CT, absence of the malignant appearance of biliary duct stenosis (*i.e.* abrupt duct cutoff or shouldering), presence of duodenal wall thickening and presence of cysts in the groove region are significantly associated with PP (P = 0.002, 0.026 and 0.001, respectively). Ishigami *et al*[17] found that a patchy enhancement pattern in the portal venous phase at CT and/or MRI is significantly associated with PP (P < 0.0001). Kalb *et al*[18] showed that poorly experienced radiologists can correctly diagnose PP at MRI with an accuracy of 87.2% (88.2% sensitivity, 86.7% specificity, 78.9% PPV, 92.9% NPV) by looking for the presence of 3 key imaging findings: Focal thickening (> 3 mm) of the second portion of the duodenum, increased enhancement of the second portion of the duodenum and cysts in the groove region. Boninsegna *et al*[22] observed that, at MRI, iso-/hypo-intensity on high b-value diffusion weighted imaging (DWI), iso-/hyper-intensity on ADC maps and delayed phase iso-/hyper-intensity are significantly associated with PP (P = 0.004, 0.005 and 0.003, respectively), as well as focal thickening of the second portion of the duodenum, presence of cysts in the groove area and absence of main pancreatic duct dilatation (P = 0.001, 0.001 and 0.005, respectively). Moreover, mean maximum diameter was significantly larger in PP than in adenocarcinoma (P = 0.0003).

DISCUSSION

Our systematic review included 14 original articles showing multimodality imaging findings in PP.

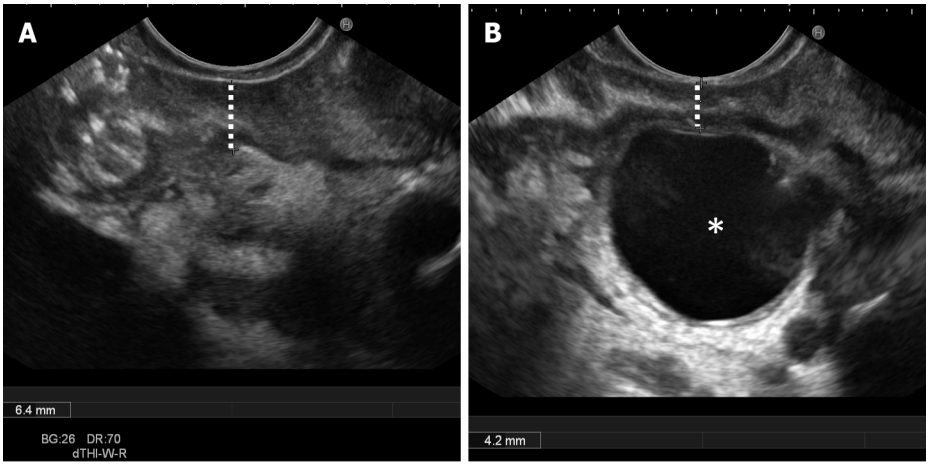

DOI: 10.4329/wjr.v15.i2.42 **Copyright** ©The Author(s) 2023.

Figure 2 Endoscopic ultrasound. A: Endoscopic ultrasound (EUS) clearly shows second duodenal portion wall thickening in a patient with chronic alcohol abuse history and abdominal pain, findings suggestive of solid subtype of paraduodenal pancreatitis; B EUS shows mild second duodenal portion wall thickening and a large duodenal wall cyst (star), findings pathognomonic for paraduodenal pancreatitis.

Imaging was the main topic in eight of the included articles, whereas it was ancillary in six of them; in these latter articles, imaging findings were not always extensively and accurately described. A total of 22 different imaging features were considered by the Authors in the included articles, with a mean of 4,4 imaging features *per* article. Surprisingly, the most frequently described imaging features were not directly correlated with PP appearance and were in the presence of main pancreatic duct dilatation (reported in 13 studies), presence of biliary duct dilatation (11 studies) and presence of pancreatic calcifications (10 studies). Presence of duodenal wall thickening and of duodenal walls cysts were also frequently assessed in the included studies (10 and 8 studies, respectively).

Typical imaging findings in PP are second duodenal portion wall thickening (88.8% of the cases), which is usually eccentric (81.8%), associated with the presence of duodenal wall cysts (82.6%) and second duodenal portion increased wall enhancement (76.3%). Duodenal wall cysts were more frequently single (65.8%) and showed a mean maximum diameter of 13 mm. The above-described imaging findings detection rates varied largely according to the adopted imaging modality. For example, duodenal wall thickening prevalence was 96.5% at EUS (Figure 2A), 91.0% at MRI and 84.1% at CT, and, similarly, duodenal wall cysts prevalence was 94.4% at EUS, 81.9% at MRI and 75.7% at CT. These differences are probably the consequence of the increased tissue contrast resolution of EUS over MRI and of MRI over CT (Figures 2B and 3). Consequently, the prevalence of cystic and solid subtypes of PP can be extremely variable and depends on the patients' population characteristics (solid subtype prevalence increases in the surgical series, given to the difficulty in differential diagnosis with pancreatic cancer, and decreases in the gastroenterological series) and from the adopted imaging modality (cystic subtype prevalence is higher in MRI and EUS series in comparison to CT series).

A solid mass in the groove region was described in less than a half (40.9%) of patients with PP. At MRI, lesion signal intensity was quite variable on T1- and T2-weighted images. On the other hand, the included lesions were hypo- to iso-intense in comparison to a normal pancreas on high b-value DWI in 100% of the cases (Figure 4A) and were iso- to hyper-intense on the ADC map in 96.4%. Therefore, the presence of increased diffusivity restriction (*i.e.* hyperintensity on high b-value DWI and hypointensity on the ADC map) has high negative predictive value for the diagnosis of PP. The solid components typically (82.4%) appeared hypovascular in the arterial phase of the dynamic study and showed a progressive enhancement during the portal venous (57.1% iso- to hyper-intense/attenuating) and the delayed (100% iso- to hyper-intense/attenuating) phases (Figure 4B). The enhancement pattern during the portal venous phase was mainly described as "patchy" (78.3% of the cases). Both patchy enhancement during portal venous phase, which is the consequence of the presence of normal pancreatic tissue between the areas of inflammatory changes[9], and delayed phase enhancement, which is the direct consequence of the presence of fibro-inflammatory tissue, are useful in the differential diagnosis between PP and pancreatic cancer.

Presence of radiological signs of obstructive chronic pancreatitis were reported with extremely variable prevalence in the included studies. For example, prevalence of main pancreatic duct dilatation ranged from 28.9% to 95.5%, prevalence of pancreatic calcifications from 20.0% to 100%, and prevalence of pancreatic cysts from 35.1% to 94.1%. The rationale of these wide differences is clearly explained in the work of de Pretis *et al*[2], which demonstrated that the prevalence of both pancreatic calcifications and main pancreatic duct dilatation significantly increases during the course of the disease. Therefore, despite the results reported by Boninsegna *et al*[22], signs of obstructive chronic pancreatitis should not be used for a differential diagnosis between PP and pancreatic cancer.

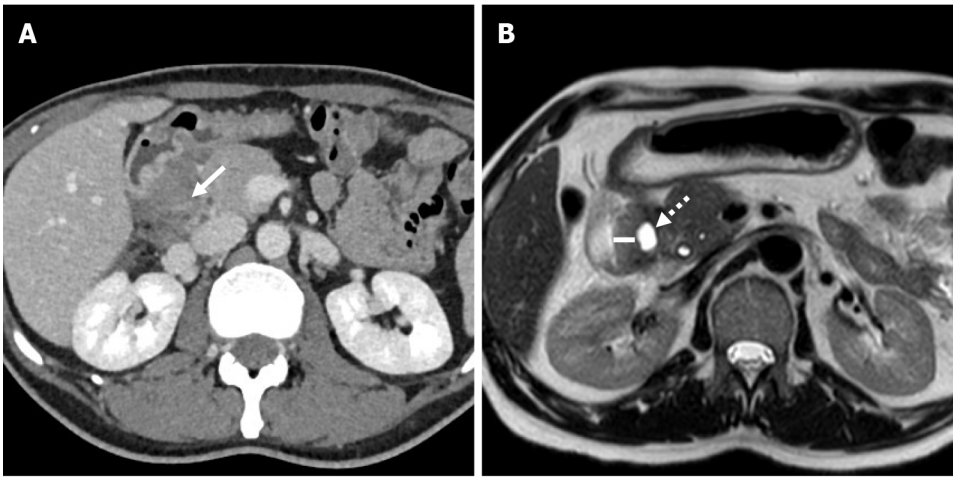

DOI: 10.4329/wjr.v15.i2.42 **Copyright** ©The Author(s) 2023.

Figure 3 A 49-year-old male patient with weight loss and abdominal pain. A: Axial 3 mm thick multiplanar reconstruction of portal venous phase computed tomography acquisition shows a hypodense mass in the groove region with patchy enhancement (arrow); B: Axial T2-weighted magnetic resonance imaging image acquired 2 mo later clearly shows eccentric second duodenal portion wall thickening (line) with cystic component (dotted arrow).

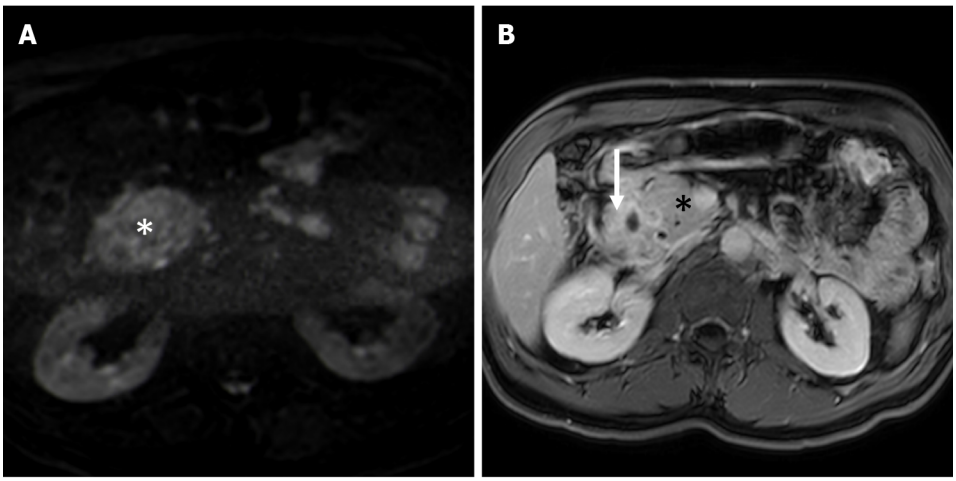

DOI: 10.4329/wjr.v15.i2.42 **Copyright** ©The Author(s) 2023.

Figure 4 Magnetic resonance imaging. A: Axial high b value (b = 800 s/mm^2) diffusion weighted imaging image shows absence of increased diffusivity restriction in the thickened groove area (star) in comparison to adjacent "normal" pancreas, finding associated with paraduodenal pancreatitis and uncommon in pancreatic cancer; B: Axial delayed phase T1-weighted magnetic resonance imaging acquisition shows increased enhancement of the duodenal walls and of the groove region (arrow) in comparison to "normal" pancreas (star), finding often associated with paraduodenal pancreatitis.

Given its expansile inflammatory nature, PP determines reactive alterations in the adjacent structures. The most frequently encountered finding was peripancreatic fat stranding, which was appreciable in 88.1% of the cases, often associated with enlarged reactive peripancreatic lymph nodes (65%). Gastroduodenal artery displacement, without infiltration or occlusion, must also be considered a common finding in PP (64.3%).

Given the central role of duodenal wall changes depiction in the differential diagnosis between PP and pancreatic cancer[21,22], MRI is mandatory if CT is inconclusive, and EUS must be performed if doubts remain even after MRI[23]. Moreover, EUS-guided fine needle aspiration/biopsy should be performed in inconclusive cases, warranting diagnostic sensitivity, specificity, positive predictive value, negative predictive value, and accuracy in differentiating PP from pancreatic cancer of 90%, 100%, 100%, 93%, and 96%, respectively[13].

The main strength of our study is that it is the first systematic literature review of imaging findings in PP. By systematically reviewing 14 different original articles dealing with imaging findings in PP, we have been able to bring together a total of 543 patients affected by PP. The article has also some weaknesses, mainly due to selection bias in the included articles and to the extreme variability of the evaluated and described imaging findings. Moreover, the differential diagnosis between PP and pancreatic cancer, which represents the main criticality, was only addressed in 4 Papers.

CONCLUSION

PP has peculiar imaging findings that enable differential diagnosis with pancreatic cancer, namely second duodenal portion eccentric wall thickening, increased enhancement, and cystic changes. Absence of increased diffusivity restriction in the groove area, patchy enhancement during the portal venous phase and delayed phase enhancement are also imaging features strongly correlated with PP. Signs of obstructive chronic pancreatitis and biliary obstruction are often present in advanced disease and must not be considered worrisome features.

CT can be considered the first line imaging modality in pancreatic pathologies and enables clinicians to perform a differential diagnosis between PP and pancreatic cancer in most of the cases. Given its higher tissue contrast resolution, MRI represents the second level imaging modality of choice in the case of inconclusive CT findings. EUS has higher accuracy than CT and MRI in depicting duodenal wall changes, offers the possibility of obtaining cyto-histologic samples, but is more invasive and less tolerated; therefore, EUS must be considered a problem-solving technique in difficult cases.

ARTICLE HIGHLIGHTS

Research background

Paraduodenal pancreatitis (PP) is a relatively rare benign inflammatory pathology that can create differential diagnosis dilemmas with pancreatic cancer. Many articles deal with imaging findings in PP, but most of them are represented by case reports, short series, or reviews.

Research motivation

The aim of our work was to perform a systematic literature review of imaging findings in PP considering only original research articles with pathology and/or clinical-radiological follow-up as the reference standard.

Research objectives

To critically describe multimodality imaging findings in PP to help clinicians in the differential diagnosis with pancreatic cancer.

Research methods

Systematic review of original articles describing imaging findings in 8 or more patients affected by PP with pathological confirmation or clinical-radiological follow-up as the gold standard.

Research results

14 articles including 543 patients were included. Computed tomography, magnetic resonance imaging (MRI) and Endoscopic ultrasound (EUS) findings were described.

Research conclusions

PP has typical findings at imaging. MRI is the most accurate radiological imaging modality, but EUS has higher sensitivity in depicting duodenal wall alterations.

Research perspectives

Radiomics features extraction may be an option in order to further increase imaging accuracy in the differential diagnosis between PP and pancreatic cancer.

FOOTNOTES

Author contributions: Bonatti M, De Pretis N and Valletta R designed the research; Bonatti M, De Pretis N, Crinò SF and Brillo A performed the research; Bonatti M, De Pretis N and Lombardo F analyzed the data; Bonatti M, Zamboni GA, Lombardo F, Mansueto G and Frulloni L wrote the paper; All authors approved the final version of the article.

Conflict-of-interest statement: All the authors report no relevant conflicts of interest for this article.

PRISMA 2009 Checklist statement: The authors have read the PRISMA 2009 Checklist, and the manuscript was prepared according to the PRISMA 2009 Checklist.

Country/Territory of origin: Italy

ORCID number: Matteo Bonatti 0000-0002-4477-8944; Nicolò De Pretis 0000-0002-3558-681X; Giulia A Zamboni 0000-0002-5059-3305; Stefano Francesco Crinò 0000-0003-4560-8741; Giancarlo Mansueto 0000-0002-1857-0613; Luca Frulloni 0000-0001-7417-2655.

S-Editor: Liu GL
L-Editor: Filipodia
P-Editor: Liu GL

REFERENCES

1 **Adsay NV**, Zamboni G. Paraduodenal pancreatitis: a clinico-pathologically distinct entity unifying "cystic dystrophy of heterotopic pancreas", "para-duodenal wall cyst", and "groove pancreatitis". *Semin Diagn Pathol* 2004; **21**: 247-254 [PMID: 16273943 DOI: 10.1053/j.semdp.2005.07.005]

2 **de Pretis N**, Capuano F, Amodio A, Pellicciari M, Casetti L, Manfredi R, Zamboni G, Capelli P, Negrelli R, Campagnola P, Fuini A, Gabbrielli A, Bassi C, Frulloni L. Clinical and Morphological Features of Paraduodenal Pancreatitis: An Italian Experience With 120 Patients. *Pancreas* 2017; **46**: 489-495 [PMID: 28196024 DOI: 10.1097/MPA.0000000000000781]

3 **Arora A**, Rajesh S, Mukund A, Patidar Y, Thapar S, Arora A, Bhatia V. Clinicoradiological appraisal of 'paraduodenal pancreatitis': Pancreatitis outside the pancreas! *Indian J Radiol Imaging* 2015; **25**: 303-314 [PMID: 26288527 DOI: 10.4103/0971-3026.161467]

4 **Frulloni L**, Gabbrielli A, Pezzilli R, Zerbi A, Cavestro GM, Marotta F, Falconi M, Gaia E, Uomo G, Maringhini A, Mutignani M, Maisonneuve P, Di Carlo V, Cavallini G; PanCroInfAISP Study Group. Chronic pancreatitis: report from a multicenter Italian survey (PanCroInfAISP) on 893 patients. *Dig Liver Dis* 2009; **41**: 311-317 [PMID: 19097829 DOI: 10.1016/j.dld.2008.07.316]

5 **Vitali F**, Hansen T, Kiesslich R, Heinrich S, Kumar A, Mildenberger P, Amodio A, Benini L, Vantini I, Frulloni L. Frequency and characterization of benign lesions in patients undergoing surgery for the suspicion of solid pancreatic neoplasm. *Pancreas* 2014; **43**: 1329-1333 [PMID: 25058888 DOI: 10.1097/MPA.0000000000000193]

6 **Balduzzi A**, Marchegiani G, Andrianello S, Romeo F, Amodio A, De Pretis N, Zamboni G, Malleo G, Frulloni L, Salvia R, Bassi C. Pancreaticoduodenectomy for paraduodenal pancreatitis is associated with a higher incidence of diabetes but a similar quality of life and pain control when compared to medical treatment. *Pancreatology* 2020; **20**: 193-198 [PMID: 31952917 DOI: 10.1016/j.pan.2019.12.014]

7 **Ooka K**, Singh H, Warndorf MG, Saul M, Althouse AD, Dasyam AK, Paragomi P, Phillips AE, Zureikat AH, Lee KK, Slivka A, Papachristou GI, Yadav D. Groove pancreatitis has a spectrum of severity and can be managed conservatively. *Pancreatology* 2021; **21**: 81-88 [PMID: 33309222 DOI: 10.1016/j.pan.2020.11.018]

8 **Casetti L**, Bassi C, Salvia R, Butturini G, Graziani R, Falconi M, Frulloni L, Crippa S, Zamboni G, Pederzoli P. "Paraduodenal" pancreatitis: results of surgery on 58 consecutives patients from a single institution. *World J Surg* 2009; **33**: 2664-2669 [PMID: 19809849 DOI: 10.1007/s00268-009-0238-5]

9 **Muraki T**, Kim GE, Reid MD, Mittal P, Bedolla G, Memis B, Pehlivanoglu B, Freedman A, Erbarut Seven I, Choi H, Kooby D, Maithel SK, Sarmiento JM, Krasinskas A, Adsay V. Paraduodenal Pancreatitis: Imaging and Pathologic Correlation of 47 Cases Elucidates Distinct Subtypes and the Factors Involved in its Etiopathogenesis. *Am J Surg Pathol* 2017; **41**: 1347-1363 [PMID: 28795998 DOI: 10.1097/PAS.0000000000000919]

10 **Vujasinovic M**, Pozzi Mucelli R, Grigoriadis A, Palmér I, Asplund E, Rutkowski W, Baldaque-Silva F, Waldthaler A, Ghorbani P, Verbeke CS, Löhr JM. Paraduodenal pancreatitis - problem in the groove. *Scand J Gastroenterol* 2022; 1-8 [PMID: 35138983 DOI: 10.1080/00365521.2022.2036806]

11 **Arvanitakis M**, Rigaux J, Toussaint E, Eisendrath P, Bali MA, Matos C, Demetter P, Loi P, Closset J, Deviere J, Delhaye M. Endotherapy for paraduodenal pancreatitis: a large retrospective case series. *Endoscopy* 2014; **46**: 580-587 [PMID: 24839187 DOI: 10.1055/s-0034-1365719]

12 **Kulkarni CB**, Moorthy S, Pullara SK, Prabhu NK. CT imaging patterns of paraduodenal pancreatitis: a unique clinicoradiological entity. *Clin Radiol* 2022; **77**: e613-e619 [PMID: 35589430 DOI: 10.1016/j.crad.2022.04.008]

13 **Jun JH**, Lee SK, Kim SY, Cho DH, Song TJ, Park DH, Lee SS, Seo DW, Kim MH. Comparison between groove carcinoma and groove pancreatitis. *Pancreatology* 2018; **18**: 805-811 [PMID: 30224296 DOI: 10.1016/j.pan.2018.08.013]

14 **Egorov VI**, Vankovich AN, Petrov RV, Starostina NS, Butkevich ATs, Sazhin AV, Stepanova EA. Pancreas-preserving approach to "paraduodenal pancreatitis" treatment: why, when, and how? *Biomed Res Int* 2014; **2014**: 185265 [PMID: 24995273 DOI: 10.1155/2014/185265]

15 **Değer KC**, Köker İH, Destek S, Toprak H, Yapalak Y, Gönültaş C, Şentürk H. The clinical feature and outcome of groove pancreatitis in a cohort: A single center experience with review of the literature. *Ulus Travma Acil Cerrahi Derg* 2022; **28**: 1186-1192 [PMID: 35920434 DOI: 10.14744/tjtes.2022.12893]

16 **Tarvainen T**, Nykänen T, Parviainen H, Kuronen J, Kylänpää L, Sirén J, Kokkola A, Sallinen V. Diagnosis, natural course and treatment outcomes of groove pancreatitis. *HPB (Oxford)* 2021; **23**: 1244-1252 [PMID: 33483260 DOI: 10.1016/j.hpb.2020.12.004]

17 **Ishigami K**, Tajima T, Nishie A, Kakihara D, Fujita N, Asayama Y, Ushijima Y, Irie H, Nakamura M, Takahata S, Ito T, Honda H. Differential diagnosis of groove pancreatic carcinomas vs. groove pancreatitis: usefulness of the portal venous

phase. *Eur J Radiol* 2010; **74**: e95-e100 [PMID: 19450943 DOI: 10.1016/j.ejrad.2009.04.026]

18 **Kalb B**, Martin DR, Sarmiento JM, Erickson SH, Gober D, Tapper EB, Chen Z, Adsay NV. Paraduodenal pancreatitis: clinical performance of MR imaging in distinguishing from carcinoma. *Radiology* 2013; **269**: 475-481 [PMID: 23847255 DOI: 10.1148/radiology.13112056]

19 **Zaheer A**, Haider M, Kawamoto S, Hruban RH, Fishman EK. Dual-phase CT findings of groove pancreatitis. *Eur J Radiol* 2014; **83**: 1337-1343 [PMID: 24935140 DOI: 10.1016/j.ejrad.2014.05.019]

20 **Wagner M**, Vullierme MP, Rebours V, Ronot M, Ruszniewski P, Vilgrain V. Cystic form of paraduodenal pancreatitis (cystic dystrophy in heterotopic pancreas (CDHP)): a potential link with minor papilla abnormalities? *Eur Radiol* 2016; **26**: 199-205 [PMID: 25991480 DOI: 10.1007/s00330-015-3799-8]

21 **Shin LK**, Jeffrey RB, Pai RK, Raman SP, Fishman EK, Olcott EW. Multidetector CT imaging of the pancreatic groove: differentiating carcinomas from paraduodenal pancreatitis. *Clin Imaging* 2016; **40**: 1246-1252 [PMID: 27636383 DOI: 10.1016/j.clinimag.2016.08.004]

22 **Boninsegna E**, Negrelli R, Zamboni GA, Tedesco G, Manfredi R, Pozzi Mucelli R. Paraduodenal pancreatitis as a mimicker of pancreatic adenocarcinoma: MRI evaluation. *Eur J Radiol* 2017; **95**: 236-241 [PMID: 28987673 DOI: 10.1016/j.ejrad.2017.08.031]

23 **Oza VM**, Skeans JM, Muscarella P, Walker JP, Sklaw BC, Cronley KM, El-Dika S, Swanson B, Hinton A, Conwell DL, Krishna SG. Groove Pancreatitis, a Masquerading Yet Distinct Clinicopathological Entity: Analysis of Risk Factors and Differentiation. *Pancreas* 2015; **44**: 901-908 [PMID: 25899649 DOI: 10.1097/MPA.0000000000000351]

Published by **Baishideng Publishing Group Inc**
7041 Koll Center Parkway, Suite 160, Pleasanton, CA 94566, USA
Telephone: +1-925-3991568
E-mail: bpgoffice@wjgnet.com
Help Desk: https://www.f6publishing.com/helpdesk
https://www.wjgnet.com